Field-Effect-Tunable Even-Odd Transition of Quantum Hall States in a Rashba System

Qijia Xu,[1,*] Jingyue Wang,[1,2,*] Junwei Huang,[3,*] Yufei Zhao,[4,*] Weiyu Sun,[1] Xuzhong Cong,[1] Huakun Zuo,[5] Zengwei Zhu,[5] Congwei Tan,[1] Hongtao Liu,[1] Binghai Yan,[4,6,†] Hongtao Yuan,[3,‡] and Hailin Peng[1,§]

[1]*Center for Nanochemistry, Beijing Science and Engineering Center for Nanocarbons, Beijing National Laboratory for Molecular Sciences, College of Chemistry and Molecular Engineering, Peking University, Beijing 100871, China*

[2]*Shandong Key Laboratory of Intelligent Energy Materials, School of Materials Science and Engineering, China University of Petroleum (East China), Qingdao 266580, China*

[3]*National Laboratory of Solid State Microstructures, Collaborative Innovation Center of Advanced Microstructures, College of Engineering and Applied Sciences, and Jiangsu Key Laboratory of Artificial Functional Materials, Nanjing University, Nanjing 210000, China*

[4]*Department of Condensed Matter Physics, Weizmann Institute of Science, Rehovot 7610001, Israel*

[5]*Wuhan National High Magnetic Field Center and School of Physics, Huazhong University of Science and Technology, Wuhan 430074, China*

[6]*Department of Materials Science and Engineering, The Pennsylvania State University, University Park, Pennsylvania 16802, USA*

(Received 8 July 2025; accepted 17 November 2025; published 9 December 2025)

The quantum Hall effect is one of the most fundamental quantum phenomena in condensed matter physics, and via tuning the quantum Hall states (QHSs), the evolution of band topologies and electron correlations can be investigated and revealed therein. However, for the vast majority of QHS systems, even- and odd-integer quantized plateaus coexist and cannot be effectively regulated. Here, we demonstrate field-effect-tunable even-odd transition of QHSs in a fixed two-unit-cell-thick (2-uc-thick) Bi_2O_2Se film, which is unlike irreversible thickness-controlled approaches [J. Wang *et al.*, Even-integer quantum Hall effect in an oxide caused by a hidden Rashba effect, Nat. Nanotechnol. **19**, 1452 (2024)]. Only even-integer quantized plateaus are observed in the 2-uc-thick epitaxial film on $SrTiO_3$ when the quantum oscillations show degenerated spin splitting under positive gate voltages. In contrast, the simultaneous emergence of even- and odd-integer QHSs is achieved under negative gate voltages, accompanied with significant spin splitting. Theoretical calculations reveal that this reversible switching stems from gate-controlled inversion symmetry breaking that modulates the splitting of Landau levels. This Letter demonstrates the significant tunability of electrostatic gating in altering inversion symmetry and modulating electron correlations in Rashba-type 2-uc-thick Bi_2O_2Se, enabling dynamic control of QHSs parity without structural changes, thereby extending the potential applications to fractional statistics and spintronics.

DOI: 10.1103/p8ds-qm44

Introduction—The quantum Hall effect (QHE) [1–17] is a macroscopic quantum phenomenon in a two-dimensional (2D) electron system, enabling the probe of band topologies and spin textures. Subjected to a sufficiently high magnetic field B, the time reversal symmetry is broken to generate Landau levels (LLs), with Zeeman splitting energy. With magnetic field varying, the Zeeman energy changes and LLs cross the Fermi surface, and the transverse resistances are quantized to plateaus of height $h/\nu e^2$ (where h is the Planck constant, e is the electron charge, and ν is an integer that represents filling factor). Crucially, this intimate connection between the filling factor and the underlying electronic band structure implies that modulating the band structure itself provides a powerful pathway to control the quantum Hall states (QHSs). One key degree of freedom for such band structure engineering in 2D systems, especially those involving heavy atoms, is the Rashba-type spin-orbit coupling (SOC). On one hand, Rashba Hamiltonian $H_{SO} = \alpha_R \boldsymbol{\sigma} \cdot (\mathbf{E} \times \boldsymbol{k})$ (where α_R is the Rashba parameter, $\boldsymbol{\sigma}$ is the Pauli metrics, $\mathbf{E}$ is the electric field perpendicular to the interface, and $\boldsymbol{k}$ is the electron wave vector) gives the separated electron pockets at the Fermi surface. On the other hand, critically for QHE control, the Zeeman splitting between LLs is strongly dependent on the Rashba SOC strength [18–21]. Therefore, this dual role of Rashba SOC is promising to effectively modulate the band structure and consequently tune the QHSs. Recently, Rashba SOC and QHE have been explored in various 2D systems, such as InSe (nanoflakes [10,22,23]), black

*These authors contributed equally to this work.

†Contact author: binghai.yan@weizmann.ac.il, binghai.yan@psu.edu

‡Contact author: htyuan@nju.edu.cn

§Contact author: hlpeng@pku.edu.cn

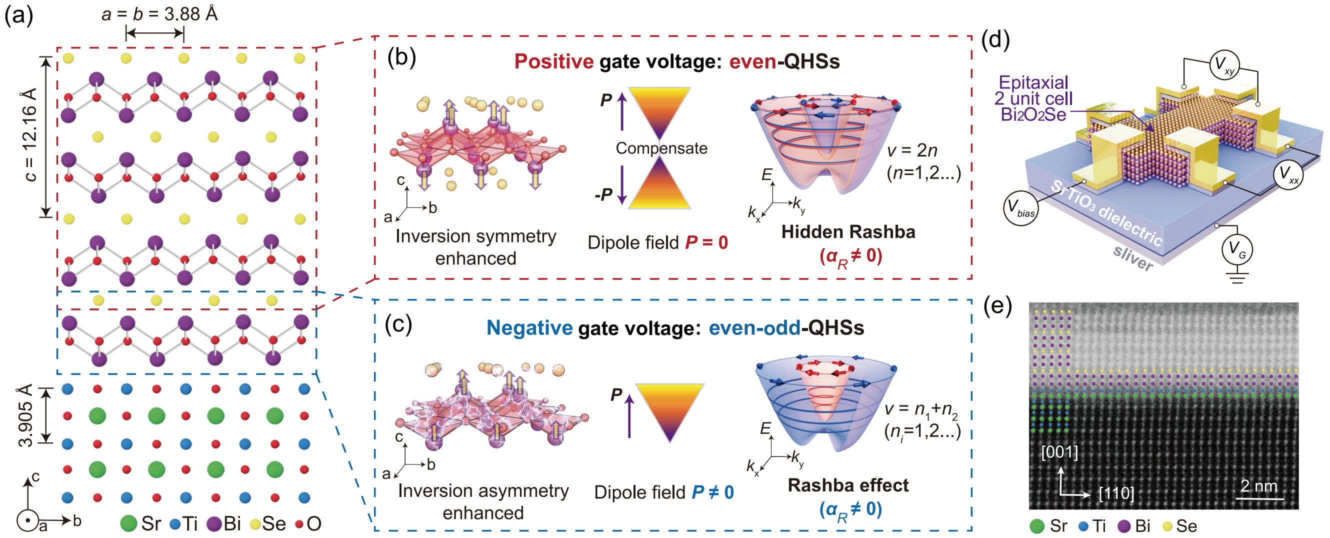

FIG. 1. Rashba-like band structure of 2-uc-thick Bi_2O_2Se film on $SrTiO_3$. (a) Lattice structure of epitaxial 2-uc-thick $Bi_2O_2Se/SrTiO_3$ heterostructure. (b) Under a positive gate voltage, inversion symmetry from bulk $[Bi_2O_2]^{2+}$ layers is enhanced, produces zero dipole field, and dominates the hidden Rashba band feature and even-integer QHSs. In the right panel, ν denotes the integer filling factor, n denotes the LL indices. (c) Under a negative gate voltage, inversion asymmetry from interfacial $[Bi_2O_2]^{2+}$ layer is enhanced, produces net dipole field, and dominates the Rashba band splitting with even- and odd-integer QHSs (n_1 and n_2 denotes the LL indices of inner and outer Fermi pocket, respectively). (d) Schematic of nonencapsulated Hall bar device fabricated by 2-uc-thick Bi_2O_2Se film; back gate is applied via a $SrTiO_3$ dielectric with silver paint. (e) Cross-sectional HAADF-STEM image of 2-uc-thick Bi_2O_2Se film. The interfacial $[TiO_2]^0$ and $[Bi_2O_2]^{2+}$ layers are completely lighted.

arsenic [3,13], and complex oxide interfaces such as $LaTiO_3/SrTiO_3$ (Refs. [24,25]), $LaAlO_3/SrTiO_3$ (Refs. [26–29]), and δ-doped $SrTiO_3$ (Ref. [8]). However, the tunable exotic quantum Hall states induced by electric field are less reported.

In this Letter, we demonstrate that the parity of QHSs in high-mobility Bi_2O_2Se (Refs. [14–16,30–34]) can be effectively tuned to switch via electrostatic gating. When a positive gate voltage is applied, only even-integer QHSs can be observed, revealing a hidden Rashba effect (Refs. [15,35]) in two-unit-cell-thick (2-uc-thick) Bi_2O_2Se, that is, the two Bi atom layers within a $[Bi_2O_2]^{2+}$ layer compensate with each other to produce a zero dipole field. In contrast, when a negative gate voltage is applied, both odd- and even-integer QHSs can be observed, as an increased internal dipole field lifts the spin degeneracy, thus leading to changes in the band topologies and spin textures. Theoretical calculations reveal a clear connection between the splitting of LLs and the global Rashba effect, which implies that by electrostatic gating, the QHSs can be effectively tuned and resolved. Hence, Zeeman splitting of LLs is modulated at same magnetic field B, exhibiting the transition of even- and odd-integer QHSs, which is of vast promise in exploring novel electron states and spintronic applications [36–41] in the future.

Rashba-like band structure and QHS transitions of 2-uc-thick Bi_2O_2Se—Bulk Bi_2O_2Se belongs to the $I4/mmm$ space group, consisting of layer-by-layer stacked tetragonal $[Bi_2O_2]^{2+}$ and $[Se]^{2-}$ layers. As shown in Figs. 1(a) and 1(e), the $[Bi_2O_2]^{2+}$ layers in 2-uc-thick $Bi_2O_2Se/SrTiO_3$ heterostructure can be divided into two types by symmetry contribution, interfacial and bulk layers. In the bulk $[Bi_2O_2]^{2+}$ layers marked by the red dashed box in Figs. 1(a) and 1(b), which preserve inversion symmetry, the upper and bottom Bi atom layers within each $[Bi_2O_2]^{2+}$ layer have opposite dipole field pointing to the adjacent $[Se]^{2-}$ layer, and their intralayer compensation results in a zero total dipole field $P = 0$. And the Rashba layers of the upper and bottom Bi atoms compensate as well to produce the degenerated Rashba bilayer structure, i.e., the hidden Rashba effect. In contrast, the interfacial $[Bi_2O_2]^{2+}$ layer marked by the blue dashed box in Figs. 1(a) and 1(c) breaks inversion symmetry due to the absence of a $[Se]^{2-}$ layer at the interface and the resultant internal dipole field $P \neq 0$, which produce the Rashba effect and lift the electron spin degeneracy.

In a previous study, a thickness-dependent relationship was established between the Rashba effect and the QHSs in Bi_2O_2Se films of varying thickness [15]. The even-integer QHSs with hidden Rashba effect exist in Bi_2O_2Se films thicker than 2.5 uc, while odd- and even-integer QHSs coexist in 1-uc-thick Bi_2O_2Se film with Rashba splitting. However, such irreversible structural control precludes real-time manipulation of electron correlations. Crucially, the 2-uc thickness, which is unexplored for electrical modulation, exhibits a critical interfacial dipole field [Figs. 1(a)–1(c)] that is tunable by field effect. Under a positive gate voltage, the inversion symmetry from the bulk $[Bi_2O_2]^{2+}$ layers is restored and dominates the band structure to be a Rashba bilayer, and the suppressed Zeeman splitting causes only even-integer QHSs. In contrast, under a negative gate voltage, the inversion asymmetry from the interfacial $[Bi_2O_2]^{2+}$ layer is enhanced and dominates the Rashba band splitting, and odd-integer QHSs emerge due to the enhanced E_z.

Firstly, in order to verify the relation of Rashba-like band structures and QHSs, we performed a pulsed high magnetic field Hall measurement with the 2-uc-thick Bi_2O_2Se film with the $SrTiO_3$ dielectric [shown in Fig. 1(d)] at 4.2 K in a pulsed high magnetic field up to 46 T. As shown in Figs. 2(a)–2(c), with a positive gate voltage $V_G = 1.2$ V, only even-integer quantum Hall plateaus (filling factors of $\nu = 8, 10, 12, 14 \ldots$) were observed in the transverse resistance (R_{xy}), with the longitudinal resistance (R_{xx}) exhibiting clear quantum oscillations due to the high carrier mobility in the 2-uc-thick epitaxial film. To determine the origin of the even-integer QHE when a positive gate voltage is applied, a fast Fourier transform (FFT) analysis of the quantum oscillations was performed, from which the band structure as well as the spin degeneracy were obtained [Fig. 2(b)]. The FFT main peak frequency $B_F = 169$ T was extracted to confirm the electron spin degeneracy because it corresponds to the carrier densities near the Fermi face ($n_{2D} = s \times B_F \times e/h$, where s is the spin degeneracy of the carrier and h is the Planck constant), and the carrier density was obtained as $s \times 4.2 \times 10^{12}$ cm^{-2}. Therefore, by comparing the carrier density to that derived from the Hall curve of approximately 9.3×10^{12} cm^{-2}, the spin degeneracy was $s = 2$. To confirm the origin of the even-integer QHSs, an inverse FFT analysis was performed and filling factors were figured out to be $v = 2n$, where n is the LL index, which is consistent with the discussion above (Supplemental Material [42] Sec. 5.1). And the band structure of the 2-uc-thick film under a positive gate voltage was further derived, as shown in Fig. 1(c), the global Rashba parameter $\alpha_R = 0$, indicating the hidden Rashba effect.

Since the dipole field from the interfacial $[Bi_2O_2]^{2+}$ layer can be enhanced further under a negative gate voltage (as discussed before), we performed an analogical electrical measurements and analyses with negative gate voltage $V_G = -1.0$ V. As shown in Fig. 2(d), both odd- and even-integer quantum Hall plateaus (filling factors of $v = 3, 4, 6, 8, 10 \ldots$) were observed in R_{xy}. The valleys of quantum oscillations were exactly matched to the quantized plateaus in R_{xy}, and additionally suggest the possible existence of $v = 5$. Similarly, an FFT analysis of the quantum oscillations was performed, and two splitting peaks with frequencies of 56 (denoted f_-) and 80 (f_+) T were obtained in the spectrum [Fig. 2(e)]. The carrier densities extracted from the FFT peak frequencies were $s \times 1.4 \times 10^{12}$ cm^{-2} and $s \times 1.9 \times 10^{12}$ cm^{-2}. Thus, by comparing the carrier density to that derived from the Hall

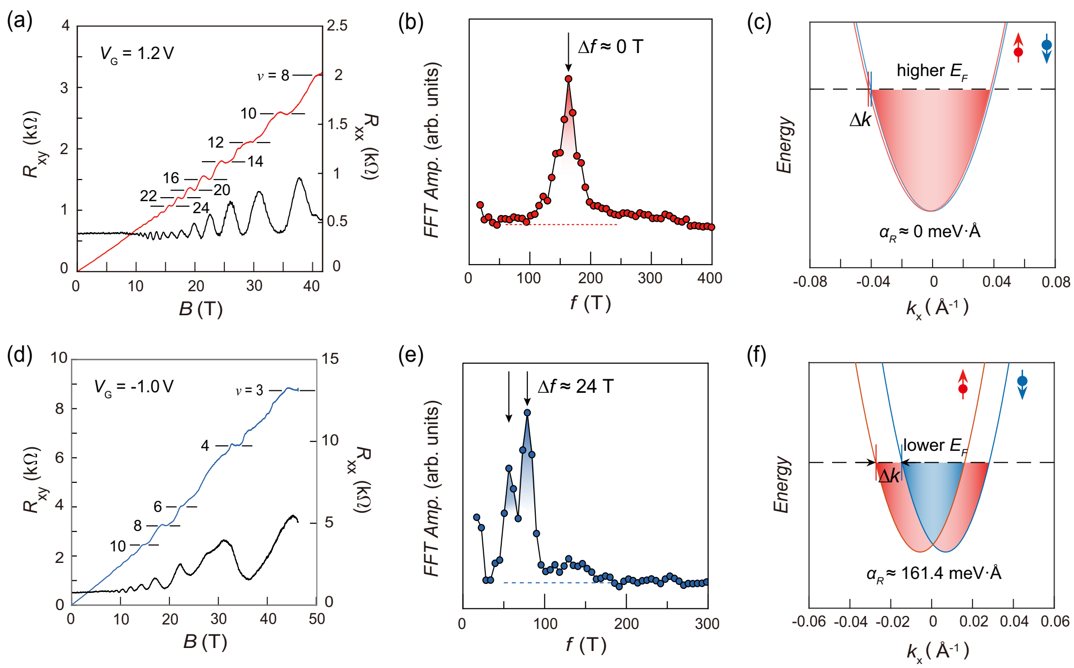

FIG. 2. Quantum Hall states and band structure in 2-uc-thick Bi_2O_2Se film with electrostatic gating. (a)–(c) The results at $V_G = 1.2$ V. (a) Even-integer QHS and quantum oscillations of the device in high magnetic field. The carrier density extracted from the slope of Hall curve is 9.3×10^{12} cm^{-2}. (b) FFT analysis of Shubnikov–de Haas (SdH) oscillations in (a). (c) Schematic of hidden Rashba band structure of 2-uc-thick Bi_2O_2Se at $V_G = 1.2$ V. (d)–(f) The results at $V_G = -1.0$ V. (d) Multiple QHSs in Hall resistance. The carrier density extracted from the slope of Hall curve is 3.9×10^{12} cm^{-2}. (e) FFT analysis of SdH oscillations in (d). (f) Schematic of Rashba splitting band structure of 2-uc-thick Bi_2O_2Se at $V_G = -1.0$ V. The different colors of band and arrows in (c) and (f) represent different spin textures. The sample was immersed in liquid helium at 4.2 K when applying the pulsed magnetic field up to 46 T.

curve of approximately 3.9×10^{12} cm^{-2}, the spin degeneracies of the two splitting peaks were $s = 1$, demonstrating Rashba splitting. The inverse FFT analyses were performed as well to confirm that the $v = 3$ plateau in R_{xy} originated from the sum of inner and outer LL indices (Supplemental Material [42] Sec. 5.2). To understand the Rashba band further, the Rashba parameter $\alpha_R = (1/m^*)\sqrt{(\hbar^3 e/2)}(\sqrt{f_+} - \sqrt{f_-}) = 161$ meV · Å was obtained, where $\hbar$ is the reduced Planck constant, m^* is the effective mass ($m^* = 0.19m_0$ from Ref. [15] and more details in Supplemental Material [42] Secs. 7 and 8).

Secondly, to study the process of band structure evolution, FFT analyses were performed for quantum oscillations [Fig. 3(a)] with gate voltages ranging from 1.2 to −1.2 V in a pulsed magnetic field. As shown in Fig. 3(b), the beating nodes, as well as Rashba splitting, decreased with a decreasing gate voltage. Finally, there existed only a single peak at $V_G = 1.2$ V, revealing no spin splitting or a net dipole field. Moreover, the ac electrical measurements and FFT analyses of the same back gate Hall device with a low magnetic field of up to 9 T at 1.7 K (see Supplemental Material [42] Sec. 6) were consistent with the high field data. As shown in Fig. 3(c), a linear evolution of Rashba parameter from 0 to 172 meV · Å was observed, highlighting the significant tunability of Rashba effect using electric gating in the 2-uc-thick Bi_2O_2Se film.

Thirdly, to visualize the transition process of even-odd-integer QHSs, R_{xx} and R_{xy} versus the gate voltage were measured by continuously tuning V_G, under fixed $T = 1.7$ K and $B = 9$ T. By plotting R_{xx} and R_{xy} together, Fig. 3(d) shows the transition of the QHSs, with each quantized plateau well matched with the quantum oscillation minima. When V_G was up to 1.0 V, only even-integer QHSs ($v = 18, 20, 22\ldots$) existed. The absence of odd-integer quantized states was due to the small Rashba parameter induced suppressed Zeeman splitting, where the electron spin was almost degenerated. While decreasing V_G, odd-integer QHS plateaus (such as $\nu = 7, 11, 13\ldots$) emerged and coexisted with even-integer QHSs ($v = 6, 8, 10\ldots$). Under these conditions, the Rashba parameter α_R increased and finally reached 172 meV · Å, and the spin degeneracy of the electron was lifted (on state). To demonstrate the stability of the transition process, V_G was swept for a cycle as well, with R_{xx} and R_{xy} behaving similarly (Supplemental Material [42] Sec. 6).

Theoretical model for the QHS transitions in 2-uc-thick Bi_2O_2Se—The emergent multiple types of QHS plateaus indicated the fermiology in 2-uc-thick Bi_2O_2Se as a competition between the hidden and global Rashba effects. In previous work [15,49], a Rashba bilayer model was built to describe the hidden Rashba effect, where we attribute opposite Rashba parameters ($\pm\alpha$) to neighboring layers. For an n-uc-thick film, we use a model including n Rashba bilayers to construct an effective Hamiltonian,

$$H = \frac{p^2}{2m^\dagger}\delta_{l,l'} + (-1)^l \frac{\alpha}{\hbar}(\sigma_x p_y - \sigma_y p_x) - t\delta_{l,l\pm1}\delta_{\sigma,\sigma'} + l\Delta\delta_{l,l'}, \quad (1)$$

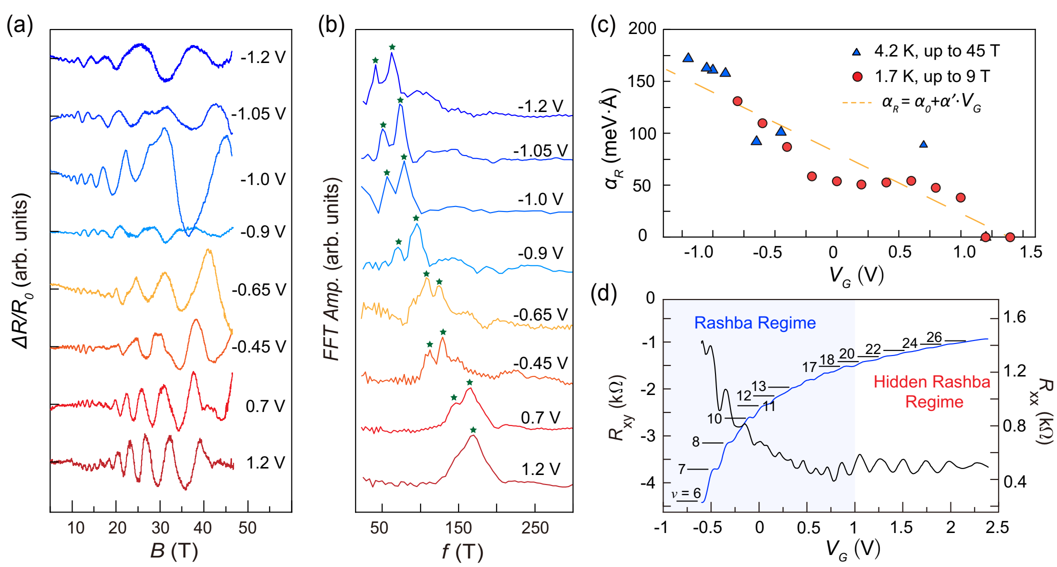

FIG. 3. Transition process of Rashba splitting and QHSs. (a) SdH oscillations of R_{xx} in 2-uc-thick Bi_2O_2Se. The curves are shifted by 200% vertically. (b) FFT analyses for each SdH oscillation in (a), showing that with gate voltage decreasing, Rashba splitting emerged and was further enhanced. The main peaks contributed to conducting electron are marked with green stars. (c) Rashba parameter extracted from the Rashba splitting in (b) and Fig. S6(b) [42], exhibiting an on-off phenomena for spin splitting. The dashed line denotes the linear fitting for the electric-field-tunable Rashba parameter. (d) Continuous QHS transition process by electrostatic gating; the QHSs could be divided into two regions: even-integer region, odd together with even-integer region. Measurements were done at 1.7 K at static magnetic fields up to 9 T.

where p is the in-plane momentum with $p^2 = p_x^2 + p_y^2$, $m^\dagger$ is the effective mass (different from m^* in the Fermi surface fitting), and the Pauli matrices σ denote spin, and $l = 1, 2, 3, 4$ is the Rashba layer index for the 2-uc film. Here, α originates from the hidden Rashba within each $[Bi_2O_2]^{2+}$ layer, distinct from the global Rashba parameter α_R, and $(-1)^l\alpha$ represents alternating Rashba effect. $l\Delta$ accounts for the potential difference between four layers, induced by the interface and external gating, resulting in inversion breaking and the global Rashba splitting in the lowest bands. If Δ vanishes, the global Rashba effect disappears. $\alpha, t, m^\dagger$ are fitted from the *ab initio* band structure. Δ and chemical potential are determined from experimentally measured Fermi surface (Fig. 2 and Supplemental [42] Sec. 8). In addition, we adopt this noninteracting model to compute LLs and neglect possible electron interactions because of the large permittivity [50] and high carrier density in the sample.

Next, a perpendicular magnetic field $\boldsymbol{B} = B\hat{z}$ and a Zeeman coupling term $(g_0\mu_B B/2)\sigma_z$ (bare Landé g factor $g_0 \approx 2$) were introduced. By selecting the Landau gauge $p \to p + eA$ with $A = (0, Bx, 0)$, the matrix elements between the nth and mth LL reads are derived,

$$H_{nm}^{ll'} = \left[\hbar\omega_c\left(n + \frac{1}{2}\right) + \frac{g_0\mu_B B}{2}\sigma_z + l\Delta\right]\delta_{nm}\delta_{ll'} + (-1)^l\delta_{ll'}\frac{\sqrt{2}\alpha}{l_B}\left(\sqrt{m}\delta_{n,m-1}\sigma^+ + \sqrt{m+1}\delta_{n,m+1}\sigma^-\right) - t\delta_{l,l'\pm1}\delta_{nm}, \tag{2}$$

where $\sigma^+ = (\sigma_x \pm i\sigma_y)/2$, $\omega_c = eB/m^*$ and $l_B = \sqrt{\hbar/eB}$ are the cyclotron frequency and magnetic length, respectively. Through the ladder operators (the second term), the hidden Rashba interaction couples different LLs. The solution relies on the intricate interplay among the Zeeman splitting, alternating Rashba SOC [represented by $(-1)^l\alpha$], and global asymmetry (introduced by Δ).

The observation of odd- and even-integer Hall plateaus relies on the splitting of LLs, since the thermal broadening can smear out the contribution from odd-integer LLs (critical value $\eta = \pi k_B T_D + 2k_B T \approx 5.34$ meV, Supplemental Material [42] Sec. 7). In the scenario with a negligible inversion breaking [$\Delta = 0$ in Fig. 4(a) when $V_G = 1.2$ V], the LL spin splitting is strongly suppressed by the hidden Rashba effect, so only even-integer plateaus are visible. Here, 8 LLs are filled near 44 T, 10 LLs near 35 T, and 12 LLs near 30 T, in excellent agreement with QHS plateaus in Fig. 2(a). In contrast, when inversion is strongly broken [$\Delta = 115$ meV in Fig. 4(b) when $V_G = -1$ V], the spin splitting increases substantially and depends on the LL index. As indicated by the green dashed line, the energy gaps between $\nu = 3$ and 4 (~6.9 meV), and between $\nu = 4$ and 5 (~10.4 meV), exceed η, allowing these QHSs to be individually resolved.

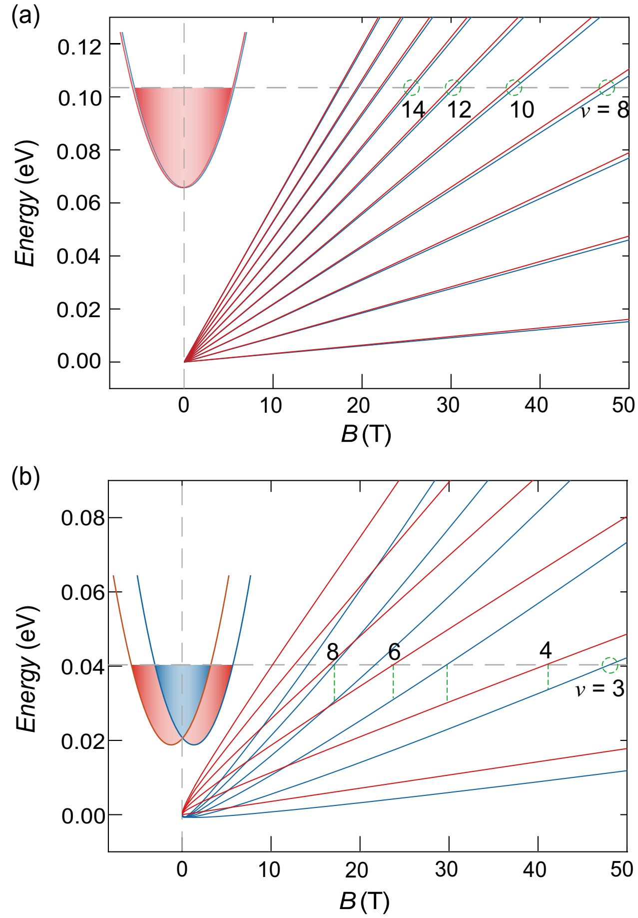

FIG. 4. Calculated Landau fan diagram (a) at gate voltage $V_G = 1.2$ V with inversion symmetry and (b) $V_G = -1.0$ V with inversion-breaking by Eq. (2). Low-energy band structures are shown in the inset. The Fermi level is marked by the horizontal gray dashed line. In (b), vertical green dashed lines mark the energy gap exceeding the thermal and disorder broadening so that even and odd QHSs can be individually identified. And the red and blue color denote the opposite spin components.

At low magnetic field, crossings between LLs reduce the effective splitting at the Fermi energy, explaining the absence of odd integers in Fig. 2(d) in the low field. Our calculations verify that the interfacial inversion symmetry is the key ingredient to control the even-odd transition of QHSs in the 2-uc-thick Bi_2O_2Se film.

Conclusion—In summary, this Letter experimentally demonstrates the electric-field-tunable SOC and even-odd transition of QHSs in the 2-uc-thick epitaxial Bi_2O_2Se film, from even-integers to the coexistence of both odd- and even-integers. The interfacial inversion asymmetry in the 2-uc-thick Bi_2O_2Se makes it an appropriate system for significantly regulating Rashba-like band structure via gate voltage induced electric fields. When applying a positive gate voltage, the inversion symmetry produces a hidden Rashba effect, where the degeneracy of the electron spin is two. In contrast, a negative gate voltage enhances the inversion asymmetry and lifts the spin degeneracy with a large Rashba splitting. When the gate voltage is decreased, the changing Rashba-like band structure results in the emergence of odd-integer QHSs, which coexist with even-integer QHSs due to the Zeeman splitting activated by large Rashba splitting. Therefore, 2-uc-thick Bi_2O_2Se with a tunable Rashba splitting and high-mobility nature could open a new avenue for manipulating spin splitting, and potentially host substantial phenomena, such as quantum spin Hall and spin-galvanic effects. Remarkably, the continuously field-effect-tunable even-odd transition of QHSs shows significant promise in the fractional quantum Hall regime to regulate the electron correlations.

Acknowledgments—This work was supported by the National Natural Science Foundation of China (T2588301 to H. P., 22432001 to H. P., 52021006 to H. P., 92164205 to J. W. and C. T., 92365203 to H. Y., U24A6002 to H. Y., and J. H., 52302180 to J. H.), the National Key Research and Development Program of China (2022YFA1204900 to H. P., 2024YFA1408104 to H. Y., 2021YFA1202901 to J. H.), Beijing National Laboratory for Molecular Sciences (BNLMS-CXTD-202001 to H. P.), the Natural Science Foundation of Jiangsu Province (BK20253012 to H. Y., BK20233001 to H. Y., BK20243011 to H. Y.). This work has been supported by the New Cornerstone Science Foundation through the New Cornerstone Investigator Program and the XPLORER PRIZE. B.Y. acknowledges the financial support from the Israel Science Foundation (ISF:2932/21, 2974/23) and the Penn State MRSEC Center for Nanoscale Science via NSF award DMR 2011839. J. W. acknowledges the support from Taishan Scholars Foundation of Shandong Province (tsqn202507115) and Qingdao Natural Science Foundation (25-1-1-195-zyyd-jch). We acknowledge Wuhan High Magnetic Field Center (WHMFC) at Huazhong University of Science and Technology, and Molecular Materials and Nanofabrication Laboratory (MMNL) in the College of Chemistry at Peking University for the use of instruments.

Data availability—The data that support the findings of this article are not publicly available. The data are available from the authors upon reasonable request.

[1] K. v. Klitzing, G. Dorda, and M. Pepper, New method for high-accuracy determination of the fine-structure constant based on quantized Hall resistance, Phys. Rev. Lett. **45**, 494 (1980).

[2] D. C. Tsui, H. L. Stormer, and A. C. Gossard, Two-dimensional magnetotransport in the extreme quantum limit, Phys. Rev. Lett. **48**, 1559 (1982).

[3] J. Hu *et al.*, Topological fermiology of gate-tunable Rashba electron gases, Sci. Adv. **10**, eadp8208 (2024).

[4] K. S. Novoselov, A. K. Geim, S. V. Morozov, D. Jiang, M. I. Katsnelson, I. V. Grigorieva, S. V. Dubonos, and A. A. Firsov, Two-dimensional gas of massless Dirac fermions in grapheme, Nature (London) **438**, 197 (2005).

[5] Y. Zhang, Y.-W. Tan, H. L. Stormer, and P. Kim, Experimental observation of the quantum Hall effect and Berry's phase in grapheme, Nature (London) **438**, 201 (2005).

[6] A. Tsukazaki, A. Ohtomo, T. Kita, Y. Ohno, H. Ohno, and M. Kawasaki, Quantum Hall effect in polar oxide heterostructures, Science **315**, 1388 (2007).

[7] L. Li *et al.*, Quantum Hall effect in black phosphorus two-dimensional electron system, Nat. Nanotechnol. **11**, 593 (2016).

[8] Y. Matsubara, K. S. Takahashi, M. S. Bahramy, Y. Kozuka, D. Maryenko, J. Falson, A. Tsukazaki, Y. Tokura, and M. Kawasaki, Observation of the quantum Hall effect in δ-doped $SrTiO_3$, Nat. Commun. **7**, 11631 (2016).

[9] Hema C. P. Movva, B. Fallahazad, K. Kim, S. Larentis, T. Taniguchi, K. Watanabe, S. K. Banerjee, and E. Tutuc, Density-dependent quantum Hall states and Zeeman splitting in monolayer and bilayer WSe_2, Phys. Rev. Lett. **118**, 247701 (2017).

[10] D. A. Bandurin *et al.*, High electron mobility, quantum Hall effect and anomalous optical response in atomically thin InSe, Nat. Nanotechnol. **12**, 223 (2017).

[11] S. Xu *et al.*, Odd-integer quantum Hall states and giant spin susceptibility in p-type few-layer WSe_2, Phys. Rev. Lett. **118**, 067702 (2017).

[12] G. Qiu, C. Niu, Y. Wang, M. Si, Z. Zhang, W. Wu, and P. D. Ye, Quantum Hall effect of Weyl fermions in n-type semiconducting tellurene, Nat. Nanotechnol. **15**, 585 (2020).

[13] F. Sheng *et al.*, Rashba valleys and quantum Hall states in few-layer black arsenic, Nature (London) **593**, 56 (2021).

[14] C. Zhang *et al.*, Single-crystalline van der Waals layered dielectric with high dielectric constant, Nat. Mater. **22**, 832 (2023).

[15] J. Wang *et al.*, Even-integer quantum Hall effect in an oxide caused by a hidden Rashba effect, Nat. Nanotechnol. **19**, 1452 (2024).

[16] O. Zheliuk *et al.*, Quantum Hall effect in a CVD-grown oxide, Nat. Commun. **15**, 10052 (2024).

[17] S. Zhao *et al.*, Fractional quantum Hall phases in high-mobility n-type molybdenum disulfide transistors, Nat. Electron. **7**, 1117 (2024).

[18] A. Manchon, H. C. Koo, J. Nitta, S. M. Frolov, and R. A. Duine, New perspectives for Rashba spin–orbit coupling, Nat. Mater. **14**, 871 (2015).

[19] A. Soumyanarayanan, N. Reyren, A. Fert, and C. Panagopoulos, Emergent phenomena induced by spin–orbit coupling at surfaces and interfaces, Nature (London) **539**, 509 (2016).

[20] F. Trier, P. Noël, J.-V. Kim, J.-P. Attané, L. Vila, and M. Bibes, Oxide spin-orbitronics: Spin–charge interconversion and topological spin textures, Nat. Rev. Mater. **7**, 258 (2021).

[21] G. Bihlmayer, P. Noël, D. V. Vyalikh, E. V. Chulkov, and A. Manchon, Rashba-like physics in condensed matter, Nat. Rev. Phys. **4**, 642 (2022).

[22] K. Yuan *et al.*, Realization of quantum Hall effect in chemically synthesized InSe, Adv. Funct. Mater. **29**, 1904032 (2019).
[23] D. Shcherbakov *et al.*, Layer- and gate-tunable spin-orbit coupling in a high-mobility few-layer semiconductor, Sci. Adv. **7**, eabe2892 (2021).
[24] M. J. Veit, R. Arras, B. J. Ramshaw, R. Pentcheva, and Y. Suzuki, Nonzero Berry phase in quantum oscillations from giant Rashba-type spin splitting in $LaTiO_3/SrTiO_3$ heterostructures, Nat. Commun. **9**, 1458 (2018).
[25] A. Ohtomo, D. A. Muller, J. L. Grazul, and H. Y. Hwang, Artificial charge-modulationin atomic-scale perovskite titanate superlattices, Nature (London) **419**, 378 (2002).
[26] A. Ohtomo and H. Y. Hwang, A high-mobility electron gas at the $LaAlO_3/SrTiO_3$ heterointerface, Nature (London) **427**, 423 (2004).
[27] A. D. Caviglia, S. Gariglio, C. Cancellieri, B. Sacepe, A. Fete, N. Reyren, M. Gabay, A. F. Morpurgo, and J. M. Triscone, Two-dimensional quantum oscillations of the conductance at $LaAlO_3/SrTiO_3$ interfaces, Phys. Rev. Lett. **105**, 236802 (2010).
[28] Q. Song, H. Zhang, T. Su, W. Yuan, Y. Chen, W. Xing, J. Shi, J. Sun, and W. Han, Observation of inverse Edelstein effect in Rashba-split 2DEG between $SrTiO_3$ and $LaAlO_3$ at room temperature, Sci. Adv. **3**, e1602312 (2017).
[29] A. El Hamdi, J.-Y. Chauleau, M. Boselli, C. Thibault, C. Gorini, A. Smogunov, C. Barreteau, S. Gariglio, J.-M. Triscone, and M. Viret, Observation of the orbital inverse Rashba–Edelstein effect, Nat. Phys. **19**, 1855 (2023).
[30] J. Wu *et al.*, High electron mobility and quantum oscillations in non-encapsulated ultrathin semiconducting Bi_2O_2Se, Nat. Nanotechnol. **12**, 530 (2017).
[31] H. Fu, J. Wu, H. Peng, and B. Yan, Self-modulation doping effect in the high-mobility layered semiconductor Bi_2O_2Se, Phys. Rev. B **97**, 241203(R) (2018).
[32] T. Tong *et al.*, Ultrahigh Hall mobility and suppressed backward scattering in layered semiconductor Bi_2O_2Se, Appl. Phys. Lett. **113**, 072106 (2018).
[33] Y. Liang *et al.*, Molecular beam epitaxy and electronic structure of atomically thin oxyselenide Films, Adv. Mater. **31**, 1901964 (2019).
[34] X. Zhou *et al.*, Step-climbing epitaxy of layered materials with giant out-of-plane lattice mismatch, Adv. Mater. **34**, 2202754 (2022).
[35] X. Zhang, Q. Liu, J.-W. Luo, A. J. Freeman, and A. Zunger, Hidden spin polarization in inversion-symmetric bulk crystals, Nat. Phys. **10**, 387 (2014).
[36] C. Chappert, A. Fert, and F. N. Van Dau, The emergence of spin electronics in data storage, Nat. Mater. **6**, 813 (2007).
[37] I. M. Miron, K. Garello, G. Gaudin, P.-J. Zermatten, M. V. Costache, S. Auffret, S. Bandiera, B. Rodmacq, A. Schuhl, and P. Gambardella, Perpendicular switching of a single ferromagnetic layer induced by in-plane current injection, Nature (London) **476**, 189 (2011).
[38] L. Liu, C.-F. Pai, Y. Li, H. W. Tseng, D. C. Ralph, and R. A. Buhrman, Spin-torque switching with the giant spin Hall effect of tantalum, Science **336**, 555 (2012).
[39] X. Lin, W. Yang, K. L. Wang, and W. Zhao, Two-dimensional spintronics for low-power electronics, Nat. Electron. **2**, 274 (2019).
[40] I. M. Miron *et al.*, Fast current-induced domain-wall motion controlled by the Rashba effect, Nat. Mater. **10**, 419 (2011).
[41] S.-H. Yang, K.-S. Ryu, and S. Parkin, Domain-wall velocities of up to 750 $m\,s^{-1}$ driven by exchange-coupling torque in synthetic antiferromagnets, Nat. Nanotechnol. **10**, 221 (2015).
[42] See Supplemental Material at http://link.aps.org/supplemental/10.1103/p8ds-qm44 for more information, which includes Refs. [15,24,26–28,33,34,43–48]. Section I introduces the sample growth by molecular beam epitaxy, device fabrication, and magnetotransport measurements. Sections 2 and 3 provide optical and atomic force microscope images of the sample, respectively. Sections 4 and 5 provide the data and inverse FFT analyses of results at the pulsed high magnetic field. Section 6 gives the results at the static magnetic field. Section 7 describes the Dingle temperature fitting at different magnetic fields, and finally, Sec. 8 shows the theoretical model and fitting.
[43] J. Wu, Y. Liu, Z. Tan, C. Tan, J. Yin, T. Li, T. Tu, and H. Peng, Chemical patterning of high-mobility semiconducting 2D Bi_2O_2Se crystals for integrated optoelectronic devices, Adv. Mater. **29**, 1704060 (2017).
[44] K. A. Müller and H. Burkard, $SrTiO_3$: An intrinsic quantum paraelectric below 4 K, Phys. Rev. B **19**, 3593 (1979).
[45] A. D. Caviglia, S. Gariglio, N. Reyren, D. Jaccard, T. Schneider, M. Gabay, S. Thiel, G. Hammerl, J. Mannhart, and J.-M. Triscone, Electric field control of the $LaAlO_3/SrTiO_3$ interface ground state, Nature (London) **456**, 624 (2008).
[46] L. Schubnikow and W. J. De Haas, A new phenomenon in the change of resistance in a magnetic field of single crystals of bismuth, Nature (London) **126**, 500 (1930).
[47] T. Ando, A. B. Fowler, and F. Stern, Electronic properties of two-dimensional systems, Rev. Mod. Phys. **54**, 437 (1982).
[48] D. Shoenberg, *Magnetic Oscillations in Metals* (Cambridge University Press, Cambridge, England, 1984).
[49] D. Kaplan, A. Stern, and B. Yan, Even integer quantum Hall effect in materials with hidden spin texture, arXiv:2406.03448.
[50] Z. Xu, J. Wang, T. Wang, W. Hu, X. Yang, and X. Lin, Huge permittivity and premature metallicity in Bi_2O_2Se single crystals, Sci. China Phys. Mech. Astron. **64**, 267312 (2021).